Wire Based Flexible Piezoelectric Sensor for Structural Health Monitoring Applications

Amine El Kacimi[1], Emmanuelle Pauliac-Vaujour[1], Joël Eymery[2]
[1] University Grenoble Alpes, CEA, LETI, MINATEC Campus, F-38054 Grenoble, France
[2] University Grenoble Alpes, CEA, INAC-SP2M, "Nanophysics and Semiconductors" group, F-38000 Grenoble, France

Abstract: We report on the modeling of flexible piezoelectric capacitive sensor based on GaN wires grown by Metal Organic Vapor Phase Epitaxy. Single crystal cone-shaped wires with hexagonal cross section are embedded within dielectric layers (parylene) in between two metal electrodes to achieve a capacitive structure. The device characteristics directly depend on growth conditions for example by tuning the wires length and the conicity angle.
This work quantifies by finite element calculation the impact of these two parameters on the voltage generation for a single wire incorporated into a thin dielectric layer.

Keywords: GaN, nanowires, sensor, flexible, piezoelectric.

1. Introduction

GaN wires have been used as active materials in flexible devices dedicated to structural health monitoring applications [1]. GaN wires can be efficiently grown by Metal Organic Vapor Phase Epitaxy (MOVPE) on sapphire substrate [2]. As growth conditions (*i.e.* time, temperature, pressure, silane flux…) can be tuned during MOVPE process, the wire geometry can vary, in terms length (L) and conicity angle (α), accordingly.
The complete device is made of thin layer of horizontal GaN wires assembled by the Langmuir-Blodgett method on a metalized flexible substrate coated by parylene [3]. The wires are encapsulated by a second parylene layer and metallic electrode to obtain a capacitive structure (Fig. 1).

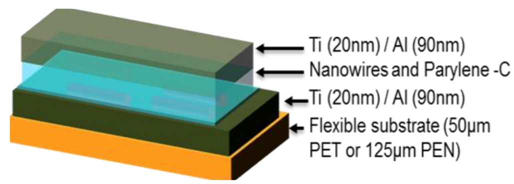

Figure 1 Schematic view of the capacitive sensor stacking [3].

2. Structure modelling:

The wire geometry is implemented in COMSOL, after it has been modeled mathematically taking into account the three adjustable parameters:

$$\begin{gathered} Wire\ length\ L \\ conicity\ angle\ \alpha \\ Top\ diameter\ R_{top} \end{gathered}$$

The wire structure is obtained from a hexagonal section extruded along the X-axis, according to a specific extrusion ratio called "f" chosen to achieve realistic shapes in agreement with microscopy observations. The c-axis and b –axis of the GaN hexagonal wurtzite structure are oriented along the x-axis and y-axis of COMSOL reference respectively. The facet of the hexagonal section therefore corresponds to experimental measurements [2]. As the phenomenon behind potential generation is surface and volume related, it was mandatory to be able to control these quantities during the parametric sweep of independent variables.

Consequently, the expression of "f" was properly computed as function of the geometry parameters, and its value is adjusted at every step of the parametric study using the refreshed values of R_top and L allowing the volume or surface to be constant.

For a parametric study on L at a constant volume:

$$fv = \frac{R_{top}}{2 \cdot L \cdot \tan\left(\frac{\alpha}{2}\right) + R_{top}}$$

$$with \quad R_{top} = \frac{R_{top_{init}}}{\sqrt{a}}$$

$$a = \frac{L}{L_{init}}$$

and for a constant surface:

$$fs = \frac{R_{top}}{2 * L * \tan\left(\frac{\alpha}{2}\right) + R_{top}}$$

$$with \quad R_{top} = \frac{R_{top_{init}}}{a}$$

Parametric studies on α have been conducted at a constant surface over volume ratio, since it was not possible, for geometrical considerations, to achieve a sweep over the angle at a constant volume without varying the structure length. Therefore, geometry was modeled differently.
Geometrical equations of the parametric study on α are given by:

$$f = \frac{-R_{top} + \sqrt{R_{top}^2 + 4 \cdot R_{top} \cdot L \cdot \tan(\frac{\alpha}{2})}}{2 \cdot L \cdot \tan(\frac{\alpha}{2})}$$

$$R_{top} = cst$$

3. Use of COMSOL multiphysics:

3.1 Device structure:

The simulated structure (see Fig 2 and Fig. 3) consists of a single cone-shaped wire with a hexagonal cross-section embedded into 2 µm parylene layer to study the impact of L and α. The Complete device with additional metallic electrode on top and bottom and with several wires will be simulated later.

Figure 2 Structure of a single cone-shaped wire with a hexagonal cross-section with a spontaneous polarization along the x-axis that corresponds to the crystallographic c-axis of the GaN lattice. The b-axis of the crystal is collinear with the y-axis of the global frame while the a-vector of the lattice forms 120° with the b-axis in the XY plane. The lattice crystallographic base is direct.

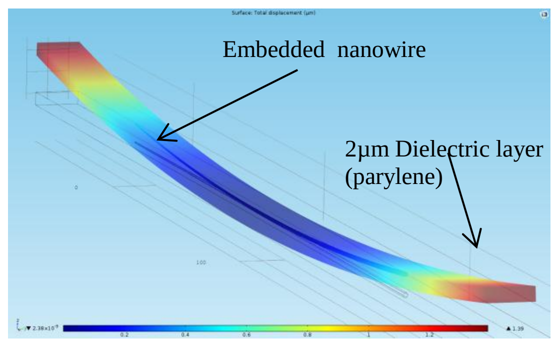

Figure 3 Device structure consisting of a single wire embedded into a parylene layer under bending.

The MEMS and "Piezoelectric devices" module were used. Wire structure was selected under "Piezoelectric material node". Constraint was applied as a prescribed displacement under Structural mechanics section. The deformation considered is a bending with a curvature radius of 10 cm. The "Ground" boundary condition was applied at the bottom face of the dielectric layer (see Fig 4).
Charge is conserved in the dielectric and piezoelectric domains. Thus, both domains were selected under "charge conservation node" with a different expression of the electric displacement field in the piezoelectric case involving the piezo polarization.

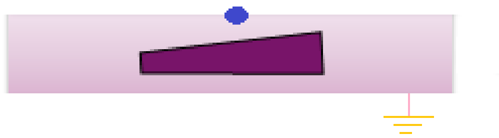

Figure 4 Schematic of a side view of the simulated structure. The blue dot indicates the region on which the potential is read.

3.2 Governing equations

Standard electrostatic equations are considered:

$$\vec{\nabla}.\vec{D} = \rho_V$$

$$\vec{E} = -\nabla V$$

With:

$$\vec{D} = \varepsilon_0 \cdot \varepsilon_r \cdot \vec{E} + P_{pze}$$

in the wire

and $$\vec{D} = \varepsilon_0 \cdot \varepsilon_r \cdot \vec{E}$$

In the dielectric material domain.

P_{pze} is piezo polarization generated by the piezoelectric effect.

4. Simulations and Results

Stationary study has been done to investigate the impact of geometry parameters on the device response under bending.
Figure 5 shows the shape of the generated potential under the previously described bending deformation. The potential was taken on the top face of the dielectric layer wrapping the wire (see Fig.4). We clearly distinguish a potential plateau along the nanowire and extrema at both extremities with opposite signs. These strong effects are resulting from the charge accumulation at the ends of the wire; indeed these surfaces correspond to the ±c-axis of the wurtzite structure [4].

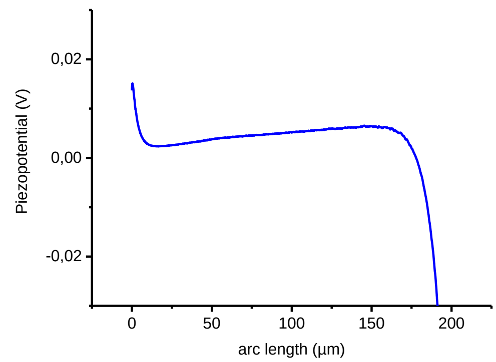

Figure 5 Potential generated by a single wire embedded into a 2µm dielectric layer under bending, for a 200 µm length wire with $\boldsymbol{R\_top = 700\,nm}$ and $\boldsymbol{alpha = 1°}$. the potential was taken on the top face of the dielectric layer along the length of the wire.

Parametric studies have been performed on L and α to understand the variation of potential plateau amplitude.

4.1 Study of the effect of wire length variation:

The parametric study on $\boldsymbol{L}$ has been performed at fixed volume and also at fixed surface. The approximate wire volume was about 68 µm^3, while the surface was about 310 µm^2. These quantities correspond to a 120 µm length wire with conical angle of 1° and 700 nm top diameter. Figure 6 shows that, at a fixed angle of 1 °, the piezo potential decreases as the nanowire gets longer, regardless fixed volume and surface. Note that starting from a typical length of about 120 µm, the two approaches are equivalent.

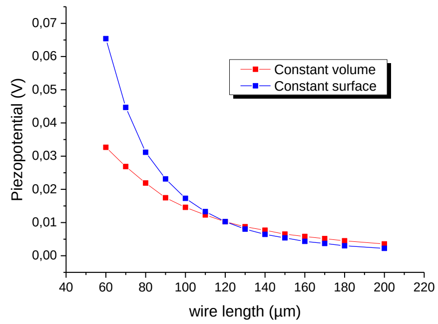

Figure 6 Piezo potential evolutions as a function of the wire length for different models, for $R_{top} = 700\ nm$ and $\alpha = 1°$. The potential is taken at the middle of the potential plateau.

The generality of the conclusions drawn from Figure 6 has been checked by estimating the volume and surface variations. Figure 7 and 8 shows very limited variations of the volume and surface respectively during the parametric sweep. These results evidence an intrinsic effect of the length variation without being influenced by volume or surface effects.

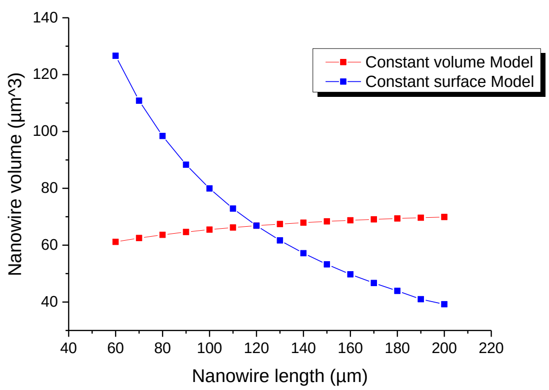

Figure 7 Wire volume evolution as function of its length for $R\_top = 700nm$ and $\alpha = 1°$.

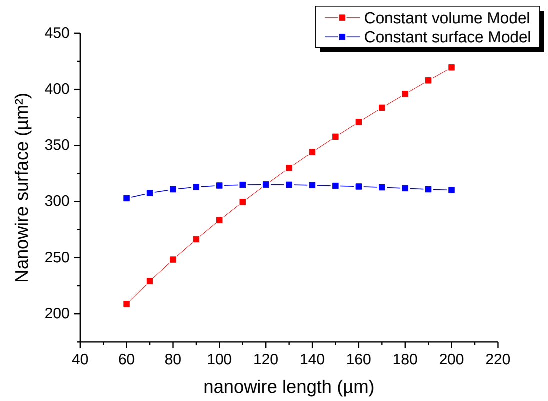

Figure 8 Wire surface evolution as function of its length for $R\_top = 700\ nm$ and $\alpha = 1°$.

4.1 Study of the effect of conicity angle variation:

Conicity variation impact has also been investigated. The importance of the conical shape has been first confirmed. The same deformation (bending with 10 cm curvature radius) has been applied to a quasi-hexagonal shape wire ($\alpha \sim 0$ °) and a conical one ($\alpha \sim 1°$). Figure 9 shows that in absence of conicity, the piezo potential measured at the plateau vanishes along the nanowire length.

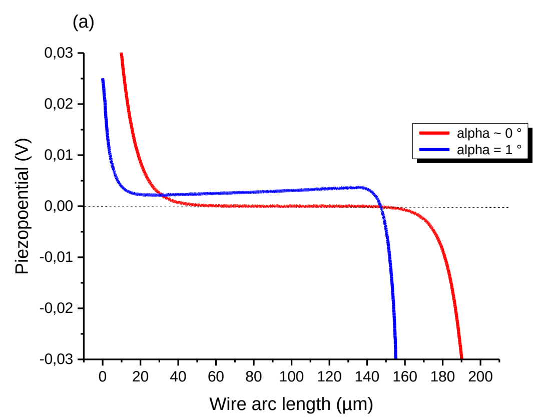

Figure 9 Piezo potential along the wire facet for a structure with $\alpha \sim 0°$ and $\alpha = 1°$.

The parametric sweep on α has been performed for different wire length as illustrated on Figure 10. We show that the impact of conicity is larger for shorter wires. Starting from the same point at 0.1° (*i.e.* nearly2 mV); at $\alpha = 2$ °, the piezo potential reaches 10 mV for $L = 50$ µm and only 4 mV for $L = 200$ µm.

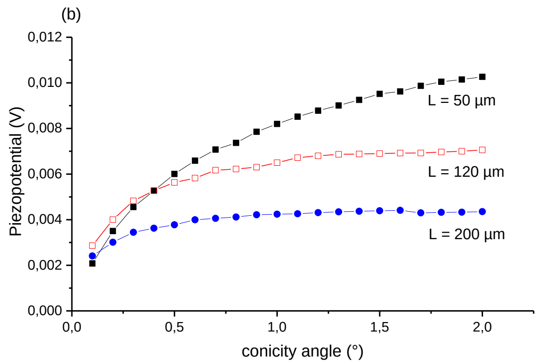

Figure 10 Piezo potential evolution as function of the conicity angle *for* $\boldsymbol{L = 50}$ µ$\boldsymbol{m}$, $\boldsymbol{L = 120}$ µ$\boldsymbol{m}$ and $\boldsymbol{L = 200}$ µ$\boldsymbol{m}$. Potential at each point was taken at the middle of the wire on the m-facet.

5. Discussions

It has been shown that short wires exhibit larger border effects as the two extremities are closer to each other. Thus, the potential peaks at the extremities get the upper hand and the potential plateau along the wire vanishes. This phenomenon makes them difficult to use in such capacitive structures.

It is therefore interesting to grow wires with length larger than ~ 50 µm to benefit from the plateau potential value that will apply to most of the surface/volume of the wire. Besides, it is not necessary to grow ultra-long wires because of potential degradation.

Simulations have also shown the importance of the conical shape for potential generation. The piezo potential vanishes for non-conical nanowires ($i.e.$ for $\alpha \sim 0$) due to the inefficiency of internal field to separate charges as pointed on Figure 11. Indeed, the Y-axis component of the piezo polarization is responsible for charge separation and accumulation onto the wire lateral facets. For non-conical structures ($\alpha = 0$) the Y-axis component of the spontaneous polarization is null and charges cannot be separated on wire facets, thus no potential is observed. Conicity is therefore mandatory for potential generation.

In addition, short nanowires are much more sensible to conicity variations than longer ones as shown on figure 10.

Nevertheless, same figure shows that a small conicity is efficient for charge separation and potential generation since potential saturation occurs starting from a certain threshold value of the angle.

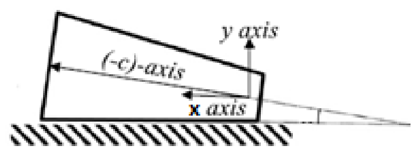

Figure 11 X and Y components of the spontaneous polarization in cone-shaped wires [2].

6. Conclusions

The significant impact of the L and alpha on wire electromechanical characteristics has been elucidated. Short wires (50 – 120 µm) with moderate conicity (<2 °) are preferred to ultra-long wires. This gives a strong indication for wire growth and device design.

It is worth mentioning that all above results were given in the specific case of the bending deformation of a single wire oriented along the c-axis. Other studies involving different types of deformations and other crystallographic orientations will be presented in further works.

7. References

1. Zhang Lin Wang, Piezotronics and Piezophotronics, Microtechnology and MEMS, pp 74-75 (2012).
2. J. Eymery et al, Self-organized and self-catalyst growth of semiconductor and metal wires by vapour phase epitaxy: GaN rods versus Cu whiskers, C. R. Physique 14, pp 221–227, (2013).

3. S. Salomon et al, GaN wire-based Langmuir–Blodgett films for self-powered flexible strain sensors, Nanotechnology 25, pp 375502, (2014)
4. O. Ambacher et al, Role of spontaneous and piezoelectric polarization induced effects in group-III nitride based heterostructures and devices.